

# Progress in Physics (21)

## Cold atoms image microwave fields

Pascal Böhi, Max F. Riedel and Philipp Treutlein  
 Departement Physik, Universität Basel, Klingelbergstrasse 82, 4056 Basel

### Introduction

Microwaves are an essential part of modern communication technology. Mobile phones and laptops, for example, are equipped with integrated microwave circuits for wireless communication and satellite navigation. In the design and development of these circuits, computer simulations play an important role. However, because of the large number of components in modern integrated circuits, such simulations have to rely on approximations and are not always reliable. Therefore, measurements are required to test the circuits and to verify their performance. To enable efficient testing and specific improvement, one would ideally like to measure all components of the microwave field directly and with very high spatial resolution.

Microwaves are difficult to detect with high resolution. In existing techniques for measuring microwaves [1], the field distribution has to be scanned point-by-point, so that data acquisition is slow. Moreover, most techniques only allow for a measurement of the amplitudes, but not of the phases of the microwave field. Furthermore, macroscopic probe heads used for the measurement can distort the microwave field and result in poor spatial resolution. We have recently developed a novel technique that avoids these drawbacks and allows for the direct and complete imaging of microwave magnetic fields with high spatial resolution [2]. In this technique, tiny clouds of laser-cooled ultracold atoms serve as non-invasive probes for the microwave field. Ultracold atoms react very sensitively to applied electromagnetic fields. Moreover, because all atoms of a given species are the same and their properties are well-known, these atomic sensors are calibrated by nature. The use of atomic gases for precision measurements has a long tradition in the field of spectroscopy and atom interferometry [3]. More recently, atoms were used for the high-resolution imaging of static magnetic and electric fields near a chip surface [4, 5].

In our experiment [2], the microwave field to be imaged drives a transition between two hyperfine states of the atoms. The probability of finding an atom in either state thereby oscillates with a Rabi frequency which depends on the local microwave

field strength at the position of the atom. After applying the microwave field for some time, its spatial field distribution is therefore imprinted onto the hyperfine state distribution in the atomic cloud. From this distribution, which we image onto a CCD-camera, we can reconstruct the microwave field.

### Description of the method

In the following, we describe our method in detail. Inside a room-temperature vacuum chamber, we place a magnetically trapped cloud of  $10^4$  laser-cooled Rubidium-87 atoms close to the microwave structure to be characterized, see Figure 1. Initially, the atoms are prepared in hyperfine sublevel  $|F=1, m_F=-1\rangle$  of the electronic ground state (Figure 1a). We switch off the trap and release the atoms to free fall. During a hold-off time  $dt_{\text{ho}}$ , the cloud drops due to gravity and expands due to its thermal velocity spread, filling the region to be imaged (Figure 1b+c). We maintain a homoge-

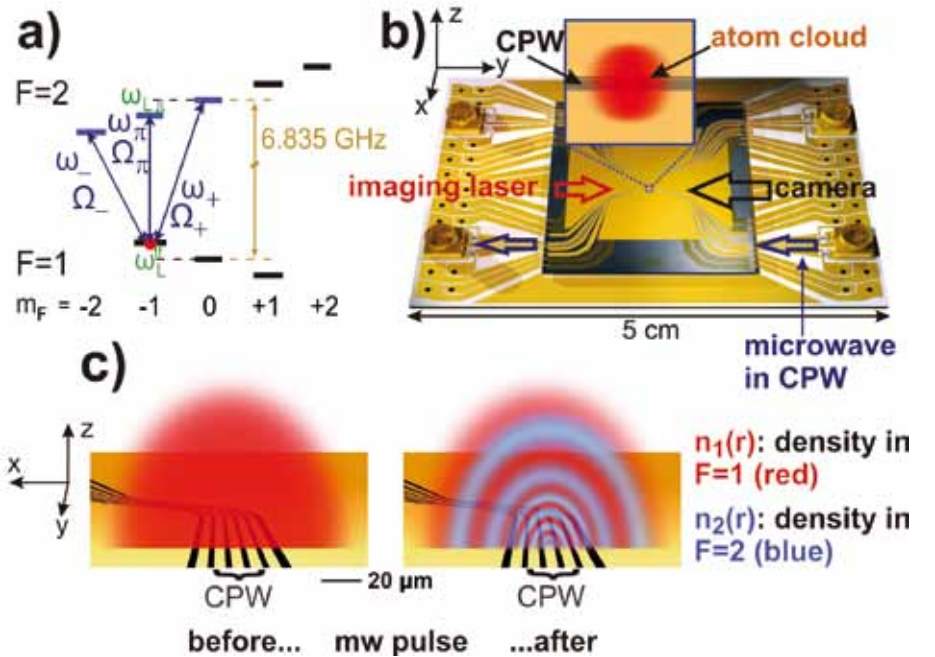


Figure 1: Illustration of the working principle of the microwave field imaging technique. (a) Ground state hyperfine levels of  $^{87}\text{Rb}$  atoms in a static magnetic field. Initially, the atoms are trapped in the hyperfine state  $|F, m_F\rangle = |1, -1\rangle$ . The three relevant transitions  $|1, -1\rangle \leftrightarrow |2, m_2\rangle$ , ( $m_2 = -2, -1, 0$ ) are indicated. The corresponding transition frequencies  $\omega_{\gamma}$  ( $\gamma = -, \pi, +$ ) are split by  $\omega_L$  due to the Zeeman effect. The resonant Rabi frequencies  $\Omega_{\gamma}$  are also indicated. (b) The atom chip used in these experiments. We note that it is not necessary to use a chip-based setup. Inset: Atom cloud near the coplanar waveguide structure (CPW) whose microwave magnetic field is examined. (c) Experimental sequence. Left: The trap is switched off and the atom cloud expands. Right: A microwave pulse is applied to the CPW, resonant with one of the transitions  $\omega_{\gamma}$ . Its magnetic field of amplitude  $\mathbf{B}(\mathbf{r})$  drives Rabi oscillations with position-dependent  $\Omega_{\gamma}(\mathbf{r})$  between  $|1, -1\rangle$  (red) and the corresponding state  $|2, m_2\rangle$  (blue). The resulting atomic density distribution  $n_1(\mathbf{r})$  ( $n_2(\mathbf{r})$ ) in  $F=1$  ( $F=2$ ) is detected.

neous static magnetic field  $\mathbf{B}_0$ , which provides the quantization axis and splits the hyperfine transition frequencies  $\omega_\gamma$  ( $\gamma = -, \pi, +$ ) by the Larmor frequency  $\omega_L = \frac{\mu_B B_0}{2\hbar}$ , see Figure 1a. When the atoms fill the region of interest, a microwave signal on the microwave circuit is subsequently switched on for a duration  $dt_{mw}$  (typically some tens of microseconds). We select one of the transitions by setting the microwave frequency to  $\omega = \omega_\gamma$ . The microwave magnetic field couples to the atomic magnetic moment and drives Rabi oscillations [6] at frequency  $\Omega_\gamma(\mathbf{r})$  on the resonant transition, with  $\Omega_\gamma(\mathbf{r}) \propto B_\gamma(\mathbf{r})$ . The Rabi frequency thus directly reflects the microwave magnetic field polarization component  $B_\gamma(\mathbf{r})$  at position  $\mathbf{r}$  that drives the transition. In particular,  $B_\pi$  is the projection of the microwave magnetic field  $\mathbf{B}$  onto  $\mathbf{B}_0$ , and  $B_\pm$  ( $B_\pm$ ) is the right (left) handed circular polarization component in the plane perpendicular to  $\mathbf{B}_0$ .

After the resonant microwave pulse, a spatial distribution of atomic populations in  $F = 1$  and  $F = 2$  results, see Figure 1c. The probability to detect an atom at position  $\mathbf{r}$  in  $F = 2$  is

$$p_2(\mathbf{r}) \equiv \frac{n_2(\mathbf{r})}{n_1(\mathbf{r}) + n_2(\mathbf{r})} = \sin^2\left[\frac{1}{2}|\Omega_\gamma(\mathbf{r})| dt_{mw}\right]$$

Here,  $n_1(\mathbf{r})$  ( $n_2(\mathbf{r})$ ) is the density of atoms in  $F = 1$  ( $F = 2$ ), which can be measured using state-selective absorption imaging [7]. Thus, the microwave field strength is imprinted onto the atomic population, which can be imaged onto a CCD camera. An overview of such images of  $p_2(\mathbf{r})$  is shown in Figure 2. The different images correspond to different mi-

crowave polarization components near the coplanar waveguide structure (CPW) that is integrated on our atom chip [8].

From  $p_2(\mathbf{r})$  we can reconstruct  $|\Omega_\gamma(\mathbf{r})|$  and thus the spatial distribution of the microwave magnetic field component  $B_\gamma(\mathbf{r})$  by measuring  $p_2(\mathbf{r})$  for different values of the microwave power  $P_{mw}$ , see Figure 3 and [2]. By measuring  $B_\pi(\mathbf{r})$  with  $\mathbf{B}_0$  oriented along x, y, and z one can reconstruct the Cartesian microwave magnetic field amplitudes  $B_x$ ,  $B_y$  and  $B_z$ . By measuring the circularly polarized components  $B_\pm$  for  $\mathbf{B}_0$  along x, y and z, it is also possible to reconstruct the spatial distribution of relative phases between  $B_x$ ,  $B_y$  and  $B_z$ . For our experimental parameters, the method provides a microwave magnetic field sensitivity of  $\sim 2 \times 10^{-8}$  T and a spatial resolution of 8  $\mu\text{m}$ , which both can be improved even further with trapped Bose-Einstein condensates [2].

## Outlook

By using an interferometric technique as described in [2], it is also possible to reconstruct the spatial distribution of the absolute phase of one of the microwave polarization components, such that the microwave magnetic field  $\mathbf{B}(\mathbf{r})$  can be fully reconstructed. While we demonstrated 2D imaging, 3D imaging slice by slice is possible, either by using a gradient in  $\mathbf{B}_0$  such that only a slice of atoms is resonant with  $\omega$ , or by using a light sheet detection technique [9], where only slices of the atoms perpendicular to the camera line

of sight are illuminated, and where one collects the fluorescence of the atoms. A further variant is to shape an atomic cloud either in the spatial density distribution or in the spatial hyperfine state distribution, prior to applying the microwave pulse, such that the atoms only undergo Rabi oscillations within a defined 2D layer.

The transition frequencies  $\omega_\gamma$  between the initial state  $|1, -1\rangle$  and the target states  $|2, m_2\rangle$  ( $m_2 = -2, -1, 0$ ) for  $^{87}\text{Rb}$  can be adjusted by change of the static magnetic field  $\mathbf{B}_0$ . They can be tuned over a range of more than 10 GHz using technical-

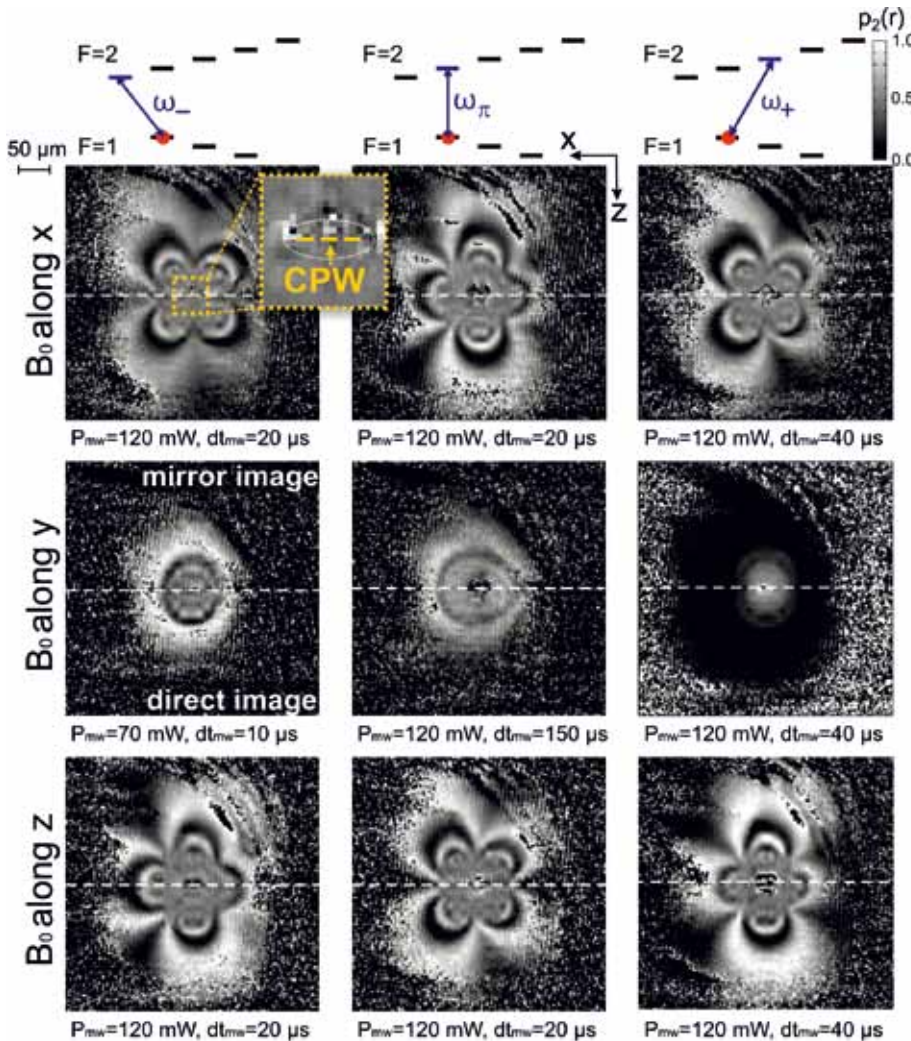


Figure 2: Imaging of microwave magnetic field components near the CPW structure. The images show the measured probability  $p_2(\mathbf{r})$  to find an atom in  $F = 2$  after applying the microwave pulse. Columns correspond to measurements on the three different transitions  $\omega_\gamma$ , rows to three different orientations of  $\mathbf{B}_0$ . The imaging beam is reflected from the chip surface at an angle of  $2^\circ$ . As a result, on each picture, the direct image and its reflection on the chip surface are visible. The dashed line separates the two. Due to distortions of the imaging beam caused by the CPW, no atoms are visible in the center. The microwave power launched into the CPW,  $P_{mw}$  and the microwave pulse duration  $dt_{mw}$  are indicated.  $dt_{ho}$  varies between 1 - 2 ms. The noise on the image periphery corresponds to regions without atoms.

ly feasible magnetic fields of up to 0.5 T. By using atomic species other than  $^{87}\text{Rb}$ , different frequency ranges become accessible, e.g. 9.2 GHz for Cs or 1.7 GHz for Na.

Our technique demonstrates the usefulness of ultracold atomic sensors for measurements of electromagnetic fields with high sensitivity and high spatial resolution. Naturally, further development is necessary before it could be used in commercial applications. In particular, it is highly desirable to further miniaturize and simplify the experimental setup required to produce and manipulate clouds of ultracold atoms. In recent years, significant progress has been made along these lines. Compact and portable systems for the preparation of ultracold atoms have been built [10], and key components of such systems are now commercially available.

- [1] S. Sayil, D. V. Kerns, and S. E. Kerns, *Potentials*, *IEEE* **24** 25-28 (2005).
- [2] P. Böhi, M. F. Riedel, T. W. Hänsch, and P. Treutlein *Appl. Phys. Lett.* **97** 051101 (2010).
- [3] A. D. Cronin, J. Schmiedmayer, and D. E. Pritchard *Rev. Mod. Phys.* **81** 1051-1129 (2009).
- [4] S. Aigner, L. Della Pietra, Y. Japha, O. Entin-Wohlman, T. David, R. Salem, R. Folman, and J. Schmiedmayer *Science* **319** 1226-1229 (2008).
- [5] J. M. Obrecht, R. J. Wild, and E. A. Cornell *Phys. Rev. A* **75** 062903 (2007).
- [6] T. R. Gentile, B. J. Hughey, D. Kleppner, and T. W. Ducas *Phys. Rev. A* **40** 5103 (1989).
- [7] M. R. Matthews, D. S. Hall, D. S. Jin, J. R. Ensher, C. E. Wieman, and E. A. Cornell *Phys. Rev. Lett.* **81** 243-247 (1998).
- [8] P. Böhi, M. F. Riedel, J. Hoffrogge, J. Reichel, T. W. Hänsch, and P. Treutlein *Nat. Phys.* **5** 592-597 (2009).
- [9] R. Bücker, A. Perrin, S. Manz, T. Betz, Ch. Koller, T. Plisson, J. Rottmann, T. Schumm, and J. Schmiedmayer *New J. Phys.* **11** 103039 (2009).
- [10] D. M. Farkas, K. M. Hudek, E. A. Salim, S. R. Segal, M. B. Squires, and D. Z. Anderson *Appl. Phys. Lett.* **96** 093102 (2010).

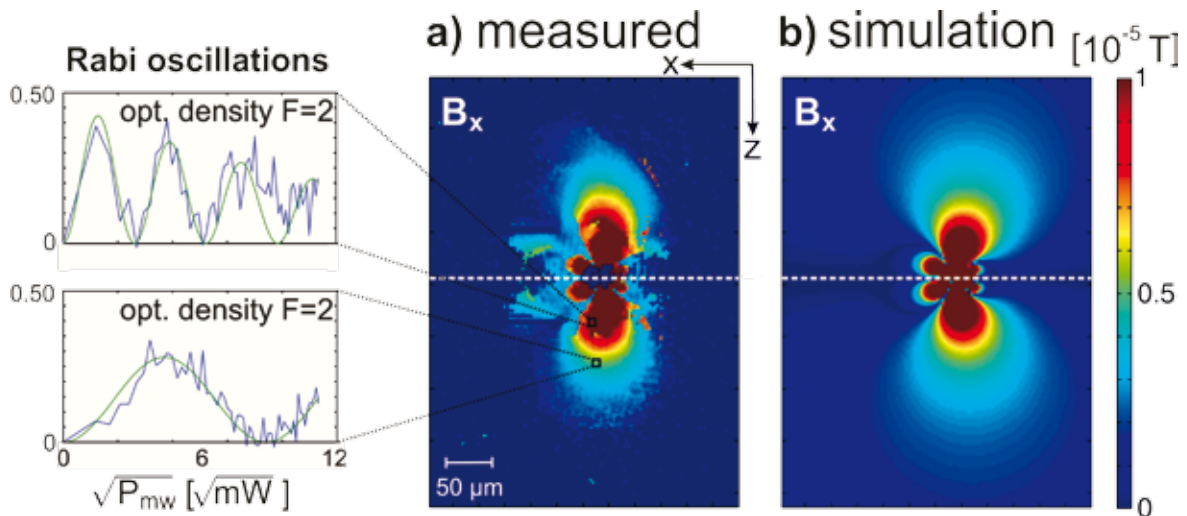


Figure 3: Extraction of the microwave magnetic field component  $B_x(\mathbf{r})$  in the vicinity of the CPW and comparison to a simulation. The dashed line separates the direct image and the reflection on the atom chip. (a) Reconstruction of  $B_x(\omega = \omega_\pi$  and  $\mathbf{B}_0$  along  $x$ ) by varying  $P_{mw}$  at fixed  $dt_{mw} = 20 \mu\text{s}$ . Shown is  $B_x(\mathbf{r})$  at  $P_{mw} = 120 \text{ mW}$  as obtained from the data. The insets show the recorded Rabi oscillations at two exemplary pixels of the image. The observed decay of the oscillations is due to microwave field gradients across the pixel. (b) Corresponding simulation of  $B_x(\mathbf{r})$  in which the microwave currents on the CPW were adjusted to reproduce the measured field distribution.

Philipp Treutlein was recently appointed as a tenure-track assistant professor in the Department of Physics at the University of Basel. Together with Pascal Böhi, Max Riedel and several other co-workers he came from LMU Munich, where the group worked previously in the laboratory of Theodor Hänsch. In Basel, the group continues its research in the field of quantum optics and ultracold atoms.

In their experiments, they use microstructured "atom chips" to laser-cool, trap, and coherently manipulate clouds of ultracold atoms. Using tailored magnetic po-

tentials generated by current-carrying wires on the chip, they perform experiments on the quantum physics of atomic Bose-Einstein condensates (BECs). In particular, they investigate many-particle entangled states of the BECs and their possible application in quantum metrology and quantum information processing. Furthermore, they use the atoms as sensitive probes for electromagnetic fields near the chip surface and to study the dynamics of on-chip solid-state systems such as tiny mechanical oscillators. One goal of these experiments is to realize hybrid quantum systems in which ultracold atoms and a solid-state system on the chip interact coherently.